X-616-68-277

PREPRINT

NASA TM X- 63270

SOLAR PLASMA FLOW PAST THE MOON

N. F. NESS
Y. C. WHANG
H. E. TAYLOR
K. W. BEHANNON

JULY 1968

GSFC — GODDARD SPACE FLIGHT CENTER
GREENBELT, MARYLAND

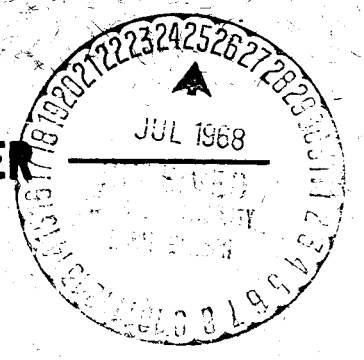

SOLAR PLASMA FLOW PAST THE MOON

N. F. Ness
Y. C. Whang*
H. E. Taylor*
K. W. Behannon

Laboratory for Space Sciences
NASA-Goddard Space Flight Center
Greenbelt, Maryland

July 1968

To be published in the Proceedings of the Sixth International Symposium on Rarefied Gas Dynamics.

*NAS-NRC Postdoctoral Associate

Extraterrestrial Physics Branch Preprint Series

ABSTRACT

Recent measurements of the magnetic field in the vicinity of the moon by Explorer 35 indicate the absence of a bow shock wave and only small perturbations in the lunar wake. A theoretical model has been developed based upon a guiding-center approximation. A favorable comparison of the theoretical and the experimental results is obtained.

I. INTRODUCTION

The solar wind represents the supersonic expansion of the solar corona into interplanetary space. It is composed primarily of protons and electrons with a small (less than 10%) admixture of doubly ionized helium and smaller amounts of heavier elements in various states of ionization. At the orbit of earth the solar wind velocity varies between 300 and 800 km/sec with a typical density of 5 protons/cm^3. This represents a proton energy of from 400 eV to 4 keV and a flux of approximately 3×10^8 protons/cm^2/sec. Imbedded in this plasma is an extended solar magnetic field of 3 to 8 γ (1 $\gamma = 10^{-5}$ oersted). In general the electron and ion temperatures are not equal and the thermal motion of the ions anisotropic. The temperature of the ions is approximately 10^5 ^oK with $T_{\parallel}/T_{\perp}$ varying between 1.5 and 4. The electron temperatures are found to be 1-3 times the ion temperatures. The length scales of interest in the solar wind vary from a collision length of the order of 1 AU to the ion gyroradius of the order of 50 km and the Debye length of the order of 10 meters. Both the Alfven and ion thermal velocities in cislunar space are approximately 50 km/sec so that the Mach number of solar wind flow is of the order of 10.

Because of the different magnetic properties of the moon and the earth, the interaction of the solar wind with these two bodies is vastly different. The main features of the earth's case (reviewed earlied in this symposium[1]) are: (i) the formation of a magnetosphere around which the bulk of the solar plasma flows, (ii) the developement of an extended magnetic tail in the antisolar direction, and (iii) the presence of a detached, collisionless bow shock wave upstream from the magnetosphere.

The adaptation of fluid flow theory to solar wind flow past the earth has been quite useful in describing this interaction. It has been especially successful in predicting the variations of the plasma and magnetic fields in the boundary layer known as the magnetosheath.

It is the purpose of this paper both to discuss recent experimental results obtained on the solar wind interaction with the moon and to present a theoretical model of this interaction based upon kinetic theory.

II. OBSERVATIONS OF MAGNETIC FIELD PERTURBATIONS BY LUNAR WAKE

The experimental results were obtained from the Explorer 35 spacecraft which was placed into a lunar orbit on July 22, 1967 with the following orbital parameters: aposelene = 5.4 Rm (Rm = 1738 km), periselene = 1.5 Rm, inclination = 169° and period = 11.5 hours.

As they orbit the earth the moon and Explorer 35 are immersed repetitively in interplanetary space, the geomagnetosheath and the geomagnetotail. Data taken while the spacecraft is in the geomagnetic tail have been used to set an upper limit to the magnetic moment of the moon[2] of 10^{20} cgs units implying a surface field of less than 4Y.

Of primary interest in this study are the periods when the moon is outside the earth's bow shock in the solar wind. During such times measurements of the magnetic field in the vicinity of the moon have been made during hundreds of spacecraft orbits. The characteristics of a bow shock (viz. a jump in field magnitude by a factor of 2-4 and substantial increase in fluctuations accompanying the heating of the plasma) have not been observed. The interplanetary magnetic field is observed to be only slightly perturbed by the presence of the moon[3-6]. In the core of the lunar wake observations characteristically show an increase of the magnetic field $\lesssim$30% of the unperturbed value. In the penumbral regions, around this core, both positive and negative perturbations of the interplanetary field strength are often observed. The magnitude and geometry of the perturbations vary with conditions in the undisturbed solar wind, verified by simultaneous measurements with other satellites in cislunar space.

The major effect of the moon on the interplanetary medium is the creation of a plasma cavity[7]; the electrons and ions impacting the surface are absorbed by the lunar body. There is also no evidence for the development of a boundary layer analogous to the earth's magnetosheath.

A sample of magnetic field measurements in the lunar wake displaying relatively large perturbations of the magnetic field is shown in Figure 1. The spacecraft trajectory is shown projected on the ecliptic plane in the upper left hand corner and positionally correlated with the data through UT annotation. As the spacecraft enters the lunar wake region, an oscillating pattern of - + - anomalies is detected. Subsequently after egression from the core region where a positive anomaly some 30% above the undisturbed field magnitude of approximately 7.5γ was detected, a set of - + - anomalies is again observed. Note that the latitude angle, θ, and longitude angle, ϕ, in selenocentric solar ecliptic coordinates, indicate the absence of appreciable directional variations of the fields through the lunar wake region.

Such large variations of the magnetic field in the lunar wake are not always observed. Figure 2 shows an example when, without the use of simultaneous correlative data from another spacecraft in cislunar space, it would have been difficult to positively identify the umbral increase. The time offset shown between the two satellites is due to their different positions in space and the structure of the interplanetary medium. Here it is noticed that only a positive anomaly of approximately 20% is readily identified in the umbral core. Other cases show even less lunar effect on the field[2,5].

These two cases are representative of the perturbations observed in the lunar wake. It is clear from multiple passes through the wake that the orientation of the interplanetary magnetic field, ϕ_o, and the ratio of plasma thermal energy to magnetic field energy, β, are important in determining both the geometry and the magnitude of the magnetic field perturbations. Interested readers are referred to the original papers for discussion of the NASA-GSFC magnetic field experiment details.

III. THEORY

1. Theoretical Model

A steady-state model for the plasma and field in the vicinity of the moon is considered here. Let $\underset{\sim}{U}_0$ denote the solar wind velocity in the unperturbed region upstream from the moon, $\underset{\sim}{B}_0$ the unperturbed magnetic field, and ϕ_0 the direction angle (the angle between $-\underset{\sim}{U}_0$ and $\underset{\sim}{B}_0$). The ratio of U_0 to the upstream ion thermal velocity is of the order of 10. The surface of the moon is assumed to absorb all impinging charged particles.

Because the Larmor radius of charged particles is small (<3%) compared with the dimension of the moon, each particle may be approximated by a guiding-center particle[8]. The lowest-order guiding-center gas has thermal motion only along the field lines[9], and thus under this approximation, the problem is reduced to the interaction between a sphere and a supersonic one-dimensional guiding-center gas. The parallel thermal motion is assumed to be maxwellian for the guiding-center gas upstream, and the magnetic moment is invariant following each guiding-center.

The velocity of a charged particle, $\underset{\sim}{V}$, may be expressed as the vector sum of the drift velocity $\underset{\sim}{u}$, the component of the guiding-center velocity parallel to the field $\underset{\sim}{v}$, and the Larmor gyrational velocity $\underset{\sim}{s}$:

$$\underset{\sim}{V} = \underset{\sim}{u} + \underset{\sim}{v} + \underset{\sim}{s}.$$

To lowest order, s is related to the magnetic moment by

$$\mu = \tfrac{1}{2} m s^2/B.$$

If a guiding-center distribution function, f, is defined as a function of v, μ, $\underset{\sim}{x}$, and t, then f is related to the ordinary distribution function F ($\underset{\sim}{V}$, $\underset{\sim}{x}$, t) by[9]

$$F \sim m\, f/2\pi B.$$

The kinetic equation can be reduced to state that f/B is conserved following the trajectory of a guiding center in phase space[10].

$$D\,(\,f/B) = 0. \qquad (1)$$

Along each trajectory the plasma is microscopically frozen into the field. In the interaction region, the guiding-center distribution function is zero if the guiding-center trajectory is intercepted by the surface of the moon. Otherwise, the frozen-in condition gives

$$f\,(\,v,\,\mu,\,\underset{\sim}{x},\,t\,) = (\,B/B_o\,)\,f\,(\,v_o,\,\mu,\,\underset{\sim}{x}_o,\,t\,). \qquad (2)$$

2. Analytical Solutions for Ion Flow

In the interaction region, the guiding-center trajectory of ions is deflected slightly from a straight line by variations of the magnetic and the electric fields. Simple analytical results for the ion flow in the interaction region are obtained in this paper by approximating the ion guiding-center trajectories by straight lines. Included in the analysis are (i) the truncation of the distribution function due to absorption of particles by the surface of the moon, and (ii) the microscopic frozen-in condition of the guiding-center plasma. This

paper presents a modification of the earlier model[8,11] by including the frozen-in condition.

Under the assumptions stated above, one can calculate the guiding-center distribution function for ions and then calculate the macroscopic flow properties[8]. The coordinate system is shown in Figure 3, the X axis is parallel to $\underset{\sim}{U}_o$, the Z axis is parallel to $\underset{\sim}{B}_o \times \underset{\sim}{U}_o$, and the origin is located at the center of the moon. The scale of the coordinate system is normalized by using the radius of the moon as a unit length. The interaction region is thus intrinsically divided into four regions as shown in Figure 3. Let $\sin^2\gamma = (1 - Z^2)/(X^2 + Y^2)$, $\tan\lambda = Y/X$ and $S^2 = U_o^2/(2kT_{\parallel o}/m_i)$. Then one can integrate the guiding-center distribution function and obtain the following results. In region 0

$$n \equiv N/N_o = B/B_o \tag{3}$$

$$p \equiv P_\parallel/P_{\parallel o} = B/B_o \tag{4}$$

In region 1

$$n = (1/2)(B/B_o)\ \mathrm{erfc}\ (\gamma_1 S) \tag{5}$$

$$p = n + S\ (B/B_o)\ \gamma_1\ \exp(-\gamma_1^2\ S^2)/\sqrt{\pi}, \tag{6}$$

where

$$\gamma_1 = \sin\ (\alpha + \lambda)/\sin(\phi_o - \alpha - \lambda),$$

and erfc is the complementary error function defined as

$$\text{erfc}\,(x) = 1 - \text{erf}\,(x) = 1 - \frac{2}{\sqrt{\pi}}\int_0^x e^{-t^2}\,dt$$

In region 2

$$n = (1/2)(B/B_0)\ \text{erfc}\,(\gamma_2 S), \tag{7}$$

$$p = n + S\,(B/B_0)\gamma_2\ \exp(-\gamma_2^2\ S^2)/\sqrt{\pi}, \tag{8}$$

where

$$\gamma_2 = \sin(\alpha - \lambda)/\sin(\Phi_0 + \alpha - \lambda).$$

In region 3

$$n = (1/2)(B/B_0)\ [\text{erfc}(\gamma_1 S) + \text{erfc}\,(\gamma_2 S)] \tag{9}$$

$$p = n + \sqrt{\frac{S}{\pi}}\left(\frac{B}{B_0}\right)\left[\gamma_1\ \exp(-\gamma_1^2 S^2) + \gamma_2\ \exp\,(-\gamma_2^2\ S^2)\right] \tag{10}$$

3. Maxwell's Equations and Numerical Solutions

Under the assumptions that the total electric current in the lunar wake[4] is composed of the magnetization current, the gradient drift current and the curvature drift current, Maxwell's equations can be written in the following dimensionless form[11],

$$\nabla \cdot \underset{\sim}{b} = 0 \tag{11}$$

$$(n + \frac{2b}{\beta})\ \underset{\sim}{\nabla} \times \underset{\sim}{b} = \underset{\sim}{b} \times \underset{\sim}{\nabla}\, n + \eta_p\, \underset{\sim}{e_1} \times (\underset{\sim}{e_1} \cdot \underset{\sim}{\nabla}\, \underset{\sim}{e_1}), \tag{12}$$

where $\underset{\sim}{b} = \underset{\sim}{B}/B_0$, $\underset{\sim}{e_1} = \underset{\sim}{b}/b$, $\beta = 8\ P_{\perp 0}/B_0^2$, and $\eta = T_{\parallel 0}/T_{\perp 0}$.

In this frozen-in model, n and p are functions of b, $\underset{\sim}{x}$, S and ϕ_0. Substituting the analystical solutions for n and p into Equations (11) and (12), one can study their solutions for n, p and $\underset{\sim}{b}$ as functions of $\underset{\sim}{x}$ and four dimensionless parameters: η, S, ϕ_0 and β. Following the method of solutions described in Reference 11, one can calculate the numerical solutions of Equations (11) and (12) on the XY-plane. Quantities obtained in a typical numerical solution are plotted as functions of the longitude angle, θ, at fixed radial distances in Figures 4 and 5. The values used for the four dimensionless parameters are also shown.

IV. SUMMARY

Experimentally the following features of the field and plasma in the wake of the moon are observed: (i) The magnitude of the magnetic field increases in the optical shadow and a pattern of alternating decreases and increases is detected at times outside the shadow[3-6]. (ii) A plasma cavity is produced in the core region of the optical shadow[7] where the field is always observed to be increased. (iii) The frozen-in condition leads to positive correlations between the ion density and magnetic field strength, i.e. $\frac{\delta B}{B_o} \approx \frac{\delta N}{N_o}$ outside the optical shadow[12]. The kinetic theory model discussed herein is generally capable of predicting these features. However, the theoretical results outside the umbral region yield perturbations of the magnetic field which are sometimes more than a factor of two smaller than the observed changes.

In addition, the present theory also predicts that only those particles with high parallel thermal energy can reach the umbral region, while the perpendicular thermal energy of particles is directly proportional to field intensity. Thus the plasma is predicted to be highly anisotropic in the lunar wake.

The explicit effects of electron flow and electric fields have been omitted. Since the flow is highly subsonic for the electrons, one expects their effects to be equivalent to use of a lower equivalent speed ratio S as they try to fill in the wake faster than the ions.

REFERENCES

1. Lazarus, A.J. "Solar Wind Flow around the Earth" presented in the Sixth International Symposium on Rarefied Gas Dynamics.

2. Behannon, K. W., NASA-GSFC preprint X-616-68-171, May 1968.

3. Ness, N.F., K.W. Behannon, C.S. Scearce and S.C. Cantarano, J. Geophys. Res., 72, 5769-5778, 1967.

4. Ness, N.F., K.W. Behannon, H.E. Taylor and Y.C. Whang, J. Geophys Res., 73, 3421-3440, 1968.

5. Colburn, D.S., R.G. Currie, J.D. Mihalov and C.P. Sonnett, Science, 158, 1040-1042, 1967.

6. Taylor, H.E., K.W. Behannon and N.F. Ness, NASA-GSFC preprint X-616-68-192, May 1968.

7. Lyon, E.F., H.S. Bridge, and J.H. Binsack, J. Geophys. Res., 72, 6113-6117, 1967.

8. Whang, Y.C., Phys. Fluids, 11, 969-975, 1968.

9. Grad, H., Electromagnetics and Fluid Dynamics of Gaseous Plasma, J. Fox, Ed. (Polytechnic Press, New York, 1961) pp. 37-64.

10. Whang, Y. C., (to be published).

11. Whang, Y. C., Phys. Fluids, 11, August 1968.

12. Siscoe, G.L., E.F. Lyon, J.H. Binsack, and H.S. Bridge, (to be published).

FIGURE CAPTIONS

Figure 1 Magnetic field measurements in lunar orbit obtained on August 7, 1967, by Explorer 35.

Figure 2 Simultaneous Explorer 33-Explorer 35 magnetic field measurements obtained on September 10, 1967.

Figure 3 Four characteristic regions of perturbed plasma flow in the vicinity of the moon.

Figure 4 Theoretical results on the plane of symmetry for $R/R_m = 3$.

Figure 5 Theoretical results on the plane of symmetry for $R/R_m = 6$.

Figure 6 A typical plot of the magnetic field topology on the plane of symmetry in the lunar wake showing the magnetic field magnitude perturbations and the plasma umbra.

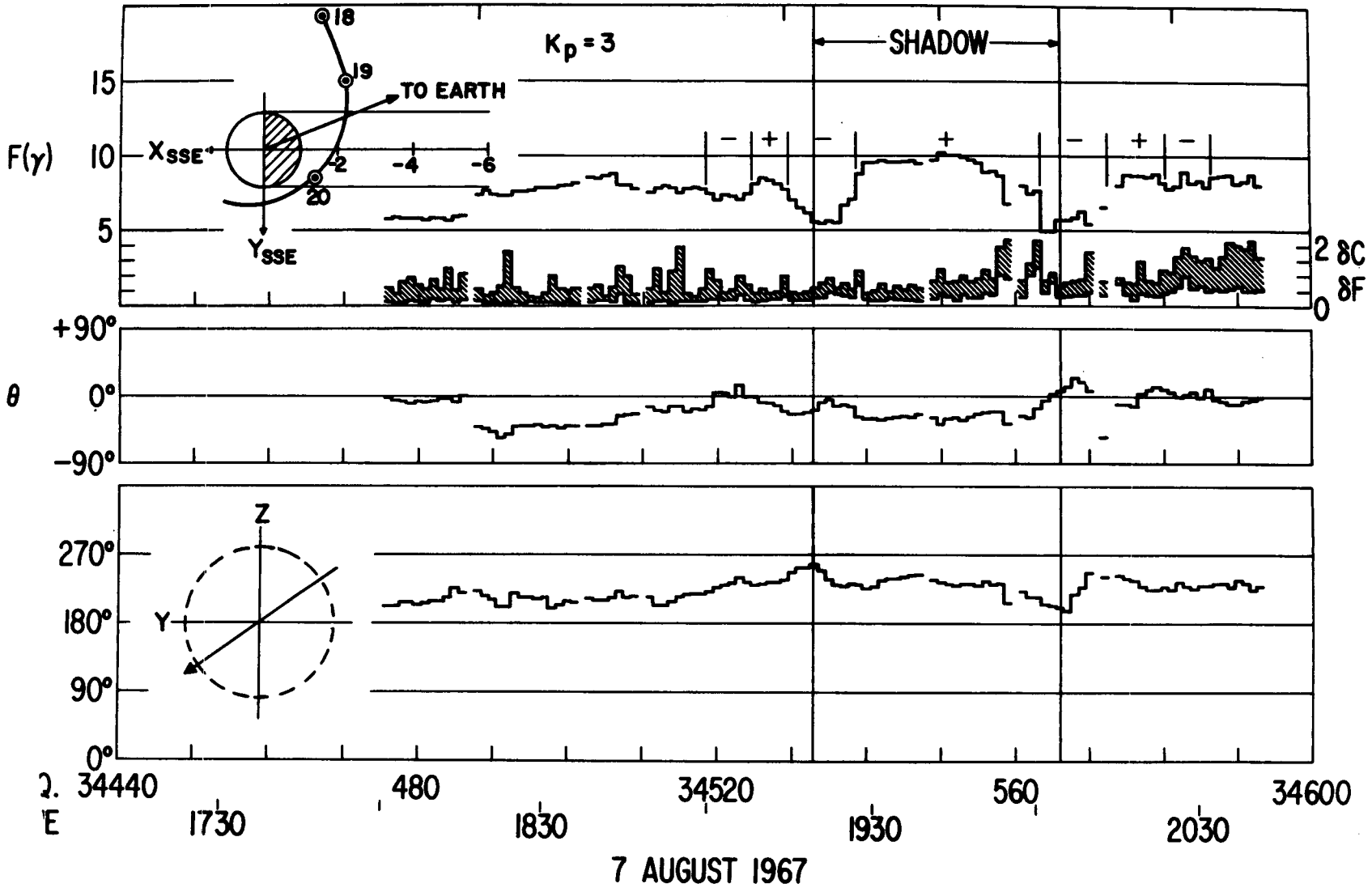
18
19
20
-2
-4
-6
TO EARTH
$K_p = 3$
SHADOW
X_{SSE}
Y_{SSE}
F(γ)
15
10
5
2 δC
0 δF
θ
+90°
0°
-90°
Z
Y
270°
180°
90°
0°
2. 34440
480
34520
560
34600
E
1730
1830
1930
2030
7 AUGUST 1967

FIGURE 1

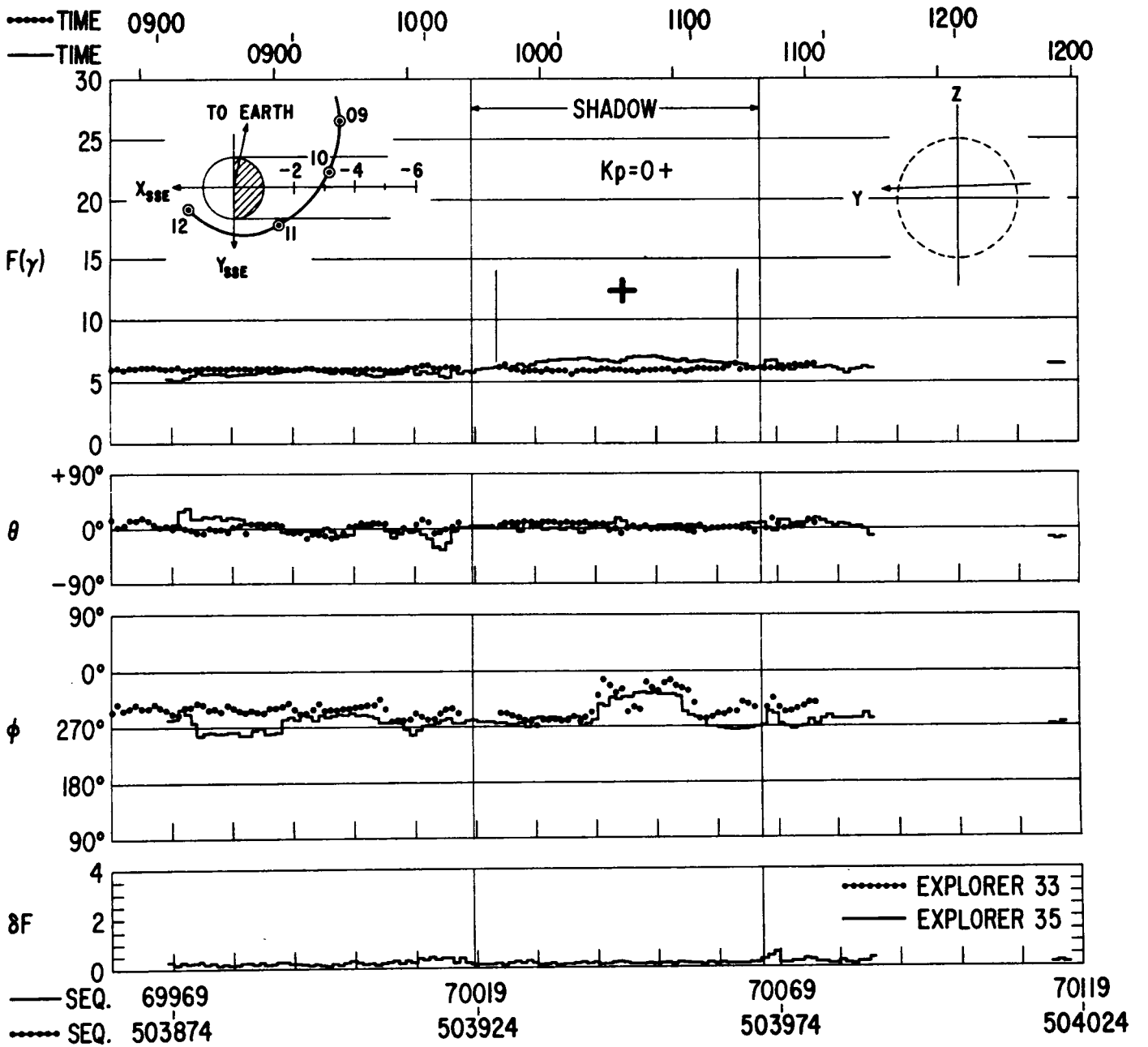

EXPLORERS 33 & 35 – 10 SEPTEMBER 1967

FIGURE 2

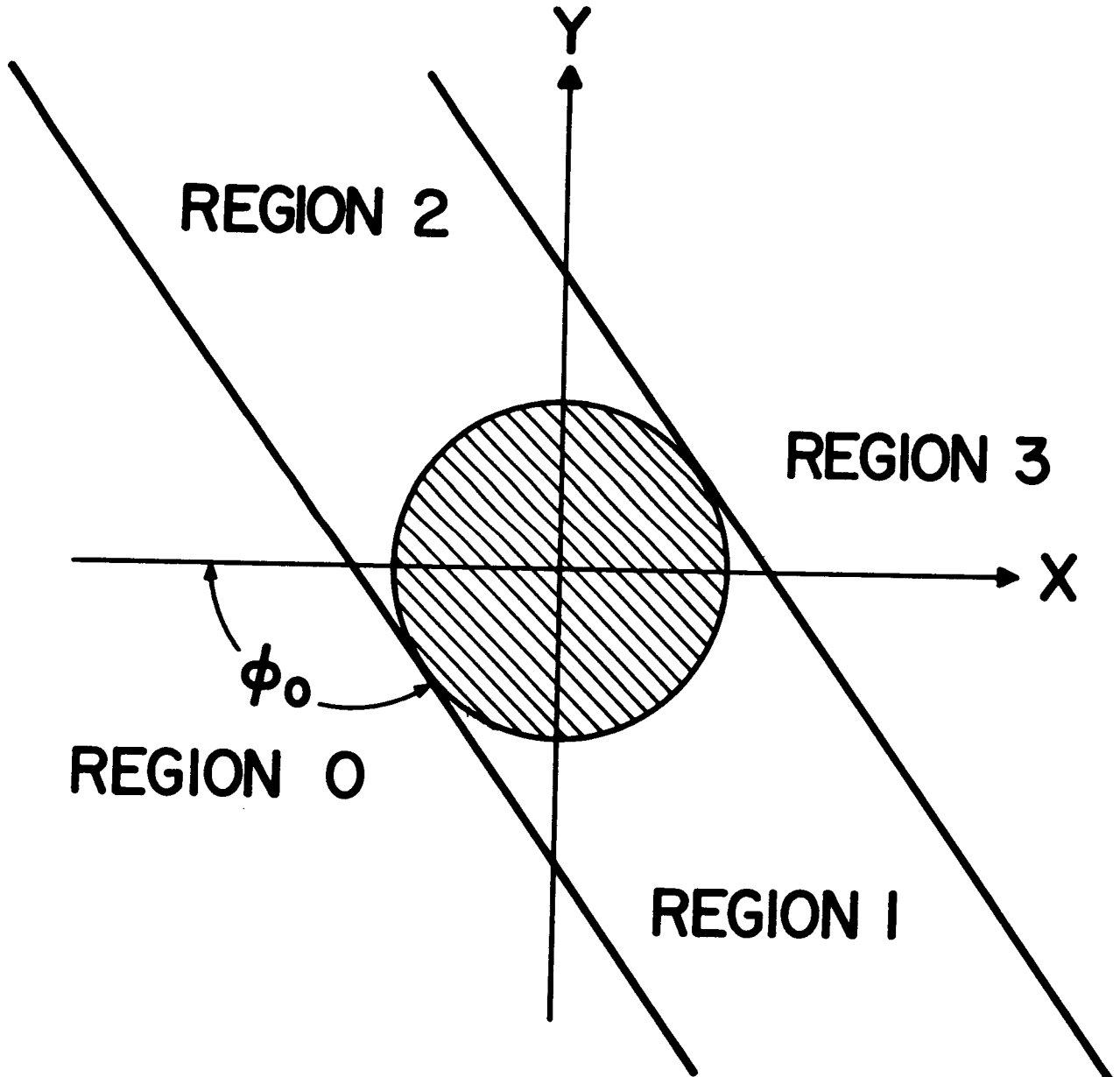

FIGURE 3

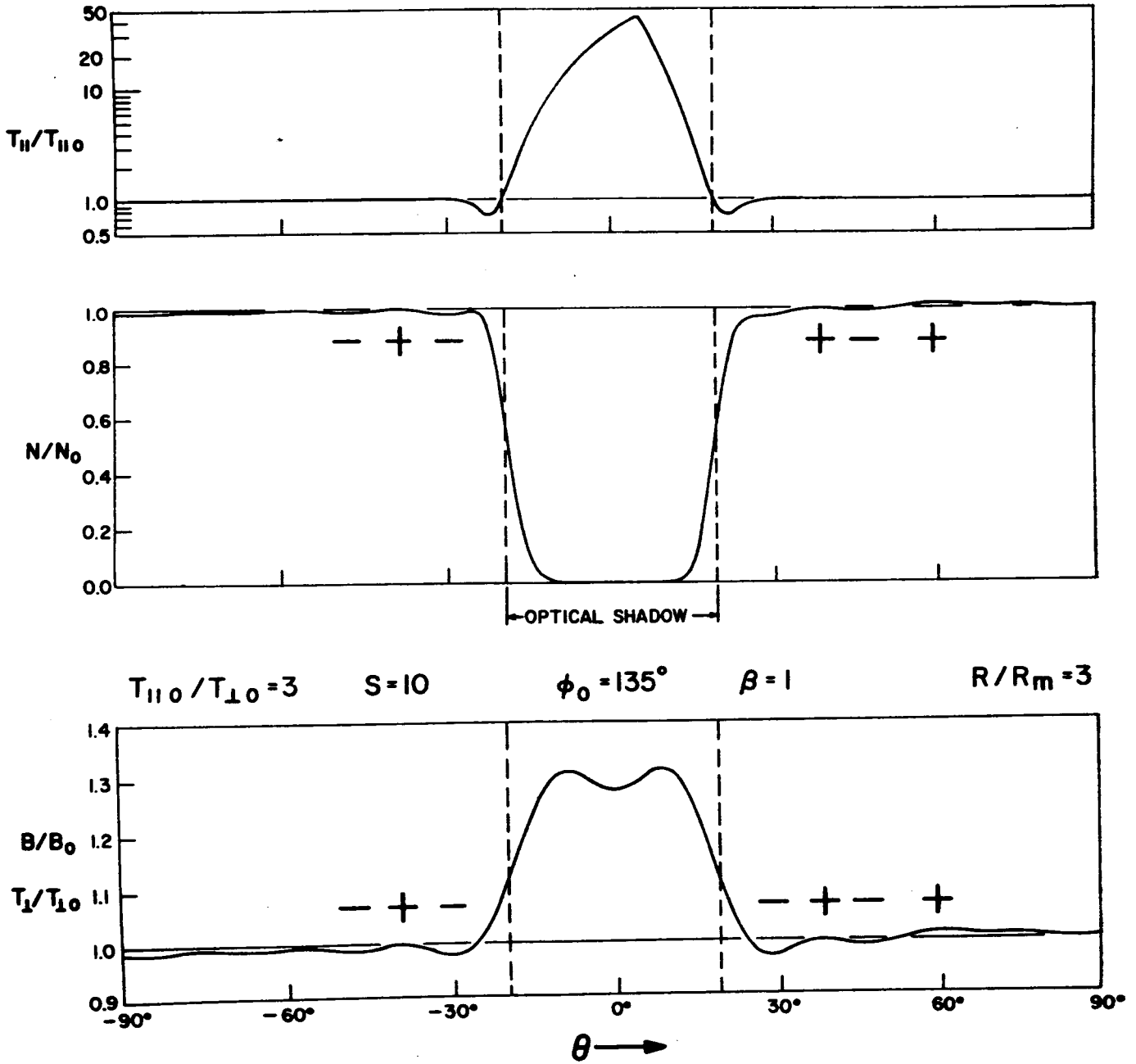
50
20
10
1.0
0.5
$T_{\parallel}/T_{\parallel 0}$
1.0
0.8
0.6
0.4
0.2
0.0
N/N_0
− + −
+ − +
OPTICAL SHADOW
$T_{\parallel 0}/T_{\perp 0}=3$
$S=10$
$\phi_0=135°$
$\beta=1$
$R/R_m=3$
1.4
1.3
1.2
1.1
1.0
0.9
B/B_0
$T_{\perp}/T_{\perp 0}$
− + −
− + − +
−90°
−60°
−30°
0°
30°
60°
90°
θ

FIGURE 4

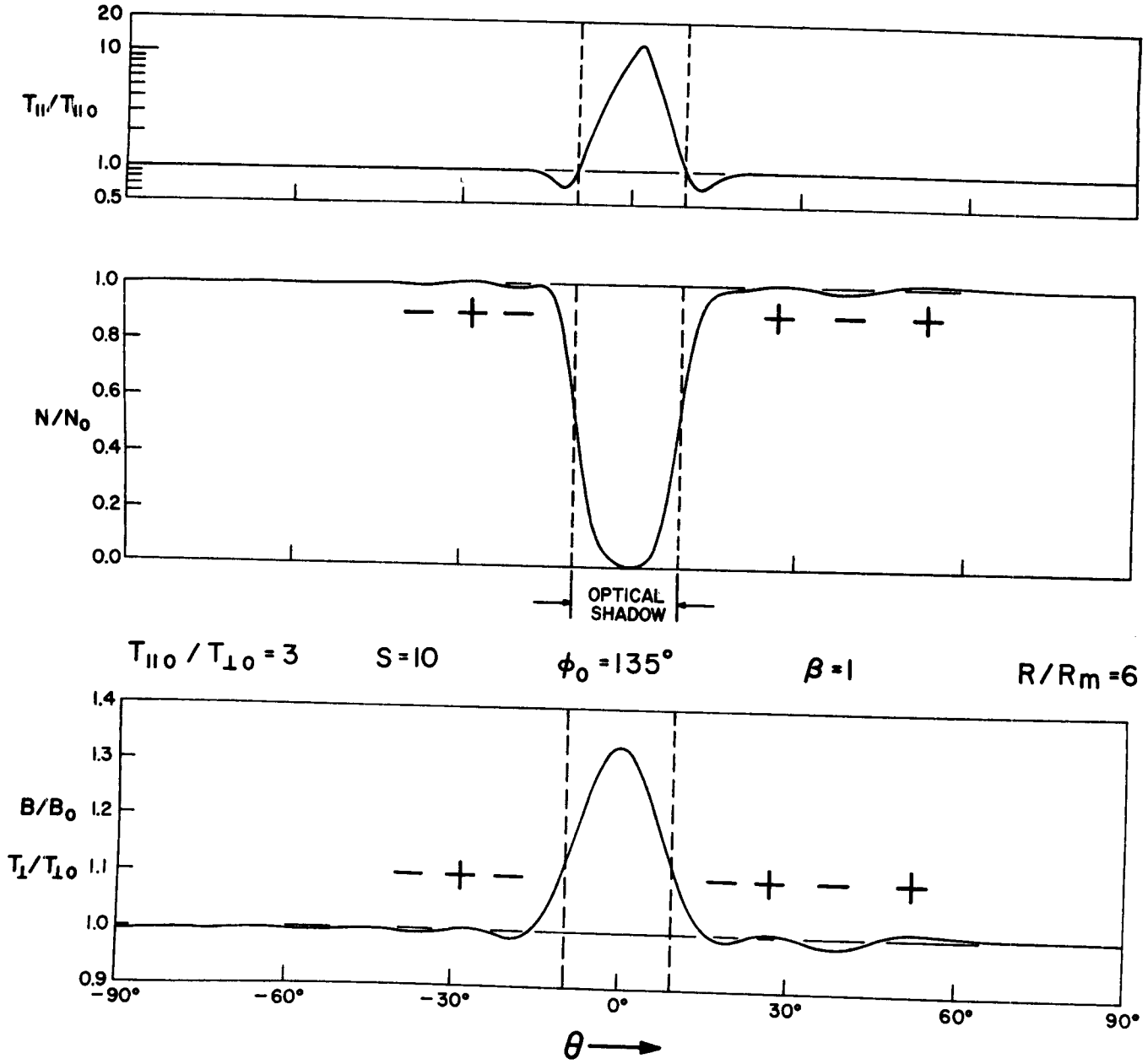
20
10
T_{11}/T_{11o}
1.0
0.5
1.0
0.8
0.6
N/N_o
0.4
0.2
0.0
− + −
+ − +
OPTICAL SHADOW
$T_{11o}/T_{\perp o} = 3$
S = 10
$\phi_o = 135°$
$\beta = 1$
$R/R_m = 6$
1.4
1.3
B/B_o
1.2
$T_\perp/T_{\perp o}$
1.1
1.0
0.9
−90°
−60°
−30°
0°
30°
60°
90°
θ

FIGURE 5

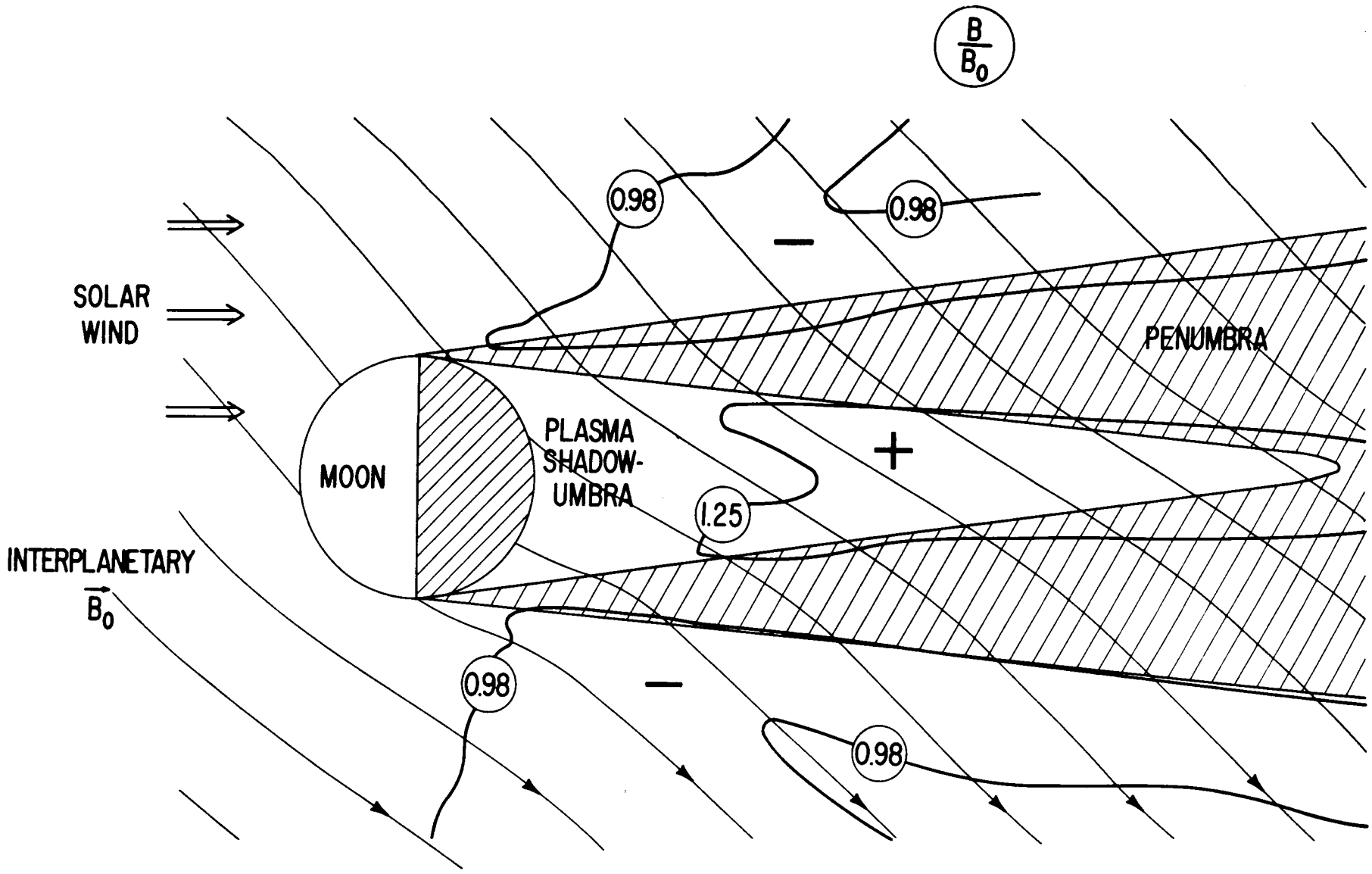
B/B0
0.98
0.98
SOLAR WIND
PENUMBRA
MOON
PLASMA SHADOW-UMBRA
1.25
INTERPLANETARY
B0
0.98
0.98

FIGURE 6